RF AND MICROWAVE ANNEALING FOR ULTRA-SHALLOW JUNCTION FORMATION

K. Thompson[1], J.H. Booske[1], D.F. Downey[2], Y. Gianchandani[1], R. Cooper[1]

1. University of Wisconsin, Madison
Madison, WI 53703

2. Varian Semiconductor Equipment Associates
Gloucester, Massachusetts 01930

Next generation, 100 nm, devices require junctions shallower than 33 nm with sheet resistances less than 600 ohms/square. A new technique for annealing implanted dopants utilizes electromagnetic fields to induce current flow through the wafer. Ohmic collisions between high-energy electrons and the lattice rapidly heats the silicon; providing the energy necessary for dopant activation. Heating rates of 125°C/sec to temperatures in excess of 1000°C have been achieved in both the RF and microwave regimes. Dopant activation experiments in an atmospheric ambient show that electromagnetic induced heating can satisfy the 100 nm device requirement and in a controlled ambient (e.g. low ppm O_2 in N_2) with optimal heating and cooling rates may meet the 70 nm requirement.

INTRODUCTION

A major obstacle for scaling to next generation, 100 nm devices is the fabrication of ultra-shallow junctions.[11] Junctions must shrink to prevent both lateral diffusion and to maintain a higher concentration of dopants in the shallow source/drain extension region. The high percentage of activated dose is necessary to maintain a contact resistance at least an order of magnitude lower than the channel resistance and to maintain junction isolation[1]. Much work has been done in this area by reducing implant depths, increasing ramp rates, and controlling the anneal ambient[2,3,4] for conventional RTA systems.

This paper introduces a novel alternative to conventional RTA systems for activating dopants during ultra shallow junction formation. This technique, known as ElectroMagnetic Induction Heating, rapidly heats silicon wafers by inducing currents to flow through the silicon; ohmically heating the entire wafer. The frequencies used varied from 13.56 MHz (RF) to microwave, 2.45 GHz. This volumetric heating contrasts with the surface heating process currently employed by conventional RTA systems. It is also speculated that the electromagnetic fields may provide an additional driving force for dopant activation. If this proves true, lower sheet resistances will be obtained at lower anneal temperatures; resulting in more efficient junctions.

EXPERIMENTAL APPARATUS

Wafer heating in the microwave regime was performed in a resonant cavity, Fig1, with radius 17 cm and a height that could be adjusted from 15 to 45 cm to tune in specific modes. In addition, a radial tuning stub helped minimize reflected power. Up to 3000 Watts of power at a frequency of 2.45 GHz was available from a magnetron source, but thus far, no more than 1350 Watts has been used. The dominant modes found were the

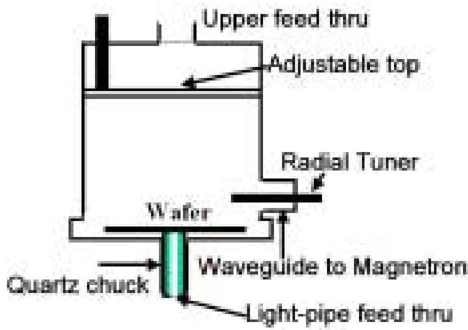

Figure 1. Schematic of the cylindrical resonant cavity used for microwave heating. The cavity is azimuthally symmetric.

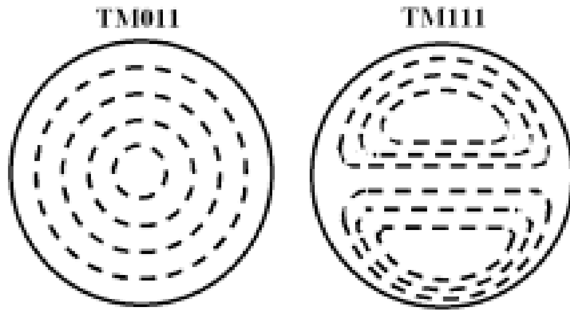

Figure 2. Magnetic field patterns in the microwave cavity for TM011 and TM111 modes in the plane of the wafer.

TM111 and TM011 whose magnetic field patterns, Fig 2, determined the current distribution and subsequent heating pattern across the wafer. Although a multi-mode resonant cavity is feasible, all experiments to date have been performed in single mode operation. The wafer was supported by a quartz chuck situated one millimeter above the bottom of the chamber (in the magnetic field maximum and electric field minimum).

Wafer heating in the RF regime was not performed in a resonant cavity but instead by exciting RF magnetic flux with a spiral copper antenna, Fig 3. Up to 1000 Watts from a fixed frequency, 13.56 MHz, power supply was matched through an L-type matching network. The wafer was positioned 2.5 cm below the coil, in the extreme near field of the antenna, on a ceramic chuck, which could be heated to 150°C if necessary.

Temperature measurement in the presence of intense electromagnetic fields poses numerous challenges as outlined in a previous publication[5]. In all experiments, temperature was measured by collecting radiated light, with an optical pyrometer or light-pipe, and sending it to a Luxtron model 10 A analyzer. The Luxtron analyzer, by matching the collected light intensities to a black body radiation spectrum, numerically deduced the temperature. The light-pipe was used for close spatial measurements, and the pyrometer was used to gather an areal average by viewing across the entire wafer.

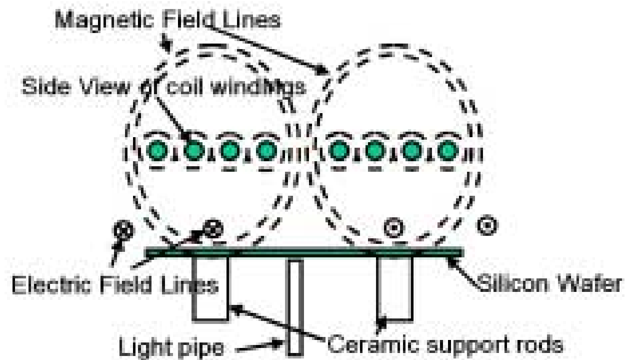

Figure 3. Schematic of RF system showing induced Magnetic and Electric field lines

In the wavelength regime of the pyrometer, the emissivity of silicon is insensitive to temperature[6], ranging between 0.65 at room temperature and 0.7 at temperatures above 700 ^{o}C. Because the pyrometer electronics assumed an emissivity of 1, the temperature measured by the pyrometer was calibrated to the solid state diffusion of boron through silicon. Several n-type, 20 ohm-cm wafers were implanted with a $10^{15}/cm^2$ dose of boron at 120 keV and annealed in a conventional furnace at several different temperatures for 15 minutes. An identically implanted wafer was heated in the microwave system at 950 Watts in the TM111 mode for 15 minutes, with a temperature of 1010 C being recorded by the lightpipe. Sheet resistance (Fig 4) and SIMS (Fig 5) analyses were performed on samples from the conventional furnace and from samples taken from the center, top (12 o'clock), and side (9 o'clock) of the microwave heated wafer.

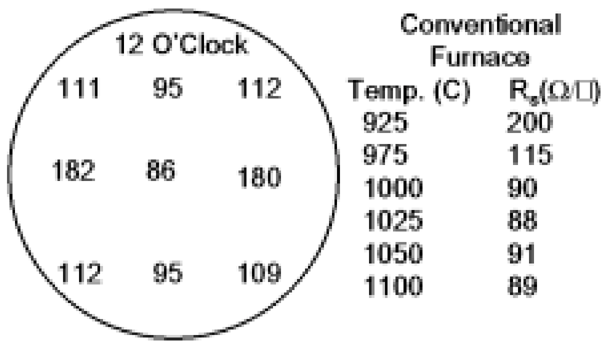

Conventional Furnace

Temp. (C)	$R_s(\Omega/\square)$
925	200
975	115
1000	90
1025	88
1050	91
1100	89

Figure 4. Sheet Resistance data from 15 minute u-wave and furnace anneals for pyrometer calibration. Statistical error +/- 5 ohm/square

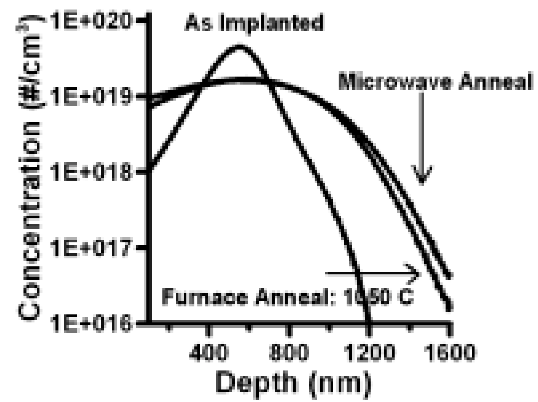

Figure 5. SIMS profiles for 15 minute u-wave and furnace anneals for pyrometer calibration.

To obtain a quantitative relationship between temperature and SIMS profile, the profiles were fit to a Gaussian curve using ORIGIN analysis software. A Gaussian profile is expected for conventional Fick's law diffusion of deep-implanted impurity ions[7]. All of the profiles fit Gaussian functions well with less than 1% deviation. The square root of the Gaussian width, obtained from this curve fit, for the furnace anneals is plotted against temperature, Fig 6. This quantity varies linearly with temperature[7], as is seen from the graph. Plotting the square root of the Gaussian widths from the microwave anneals on the same graph, one can establish the actual temperature of the wafer being heated in the microwave system. In the center this is 1060°C, at the top 1025°C, and at the edge 925°C. Overlaying the SIMS profiles, Fig 5, from the center of the microwave annealed wafer and the 1050°C furnace anneal, it is evident, from the slightly increased diffusion, that the microwave annealed wafer was indeed at a temperature slightly higher than 1050°C. Furthermore, the sheet resistances obtained from the microwave anneal agree well with those from the furnace anneals. Because the samples were annealed for a long time (15 minutes), dopant activation should be near 100% for all samples. This indicates that sheet resistance should be dependent primarily on junction depth and not be obscured by partially activated dopant concentrations. Because the temperature of the silicon wafer recorded by the light-pipe in the center of the wafer was 1010°C, it was determined that an under measurement of the temperature by ~ 5% had occurred. This amount of under measurement due to the emissivity agrees with curves provided in the Luxtron operating manual[7]. Consequently, all temperature data from the pyrometer in the temperature range of 800°C – 1100°C will be multiplied by 1.05 to account for the emissivity of silicon.

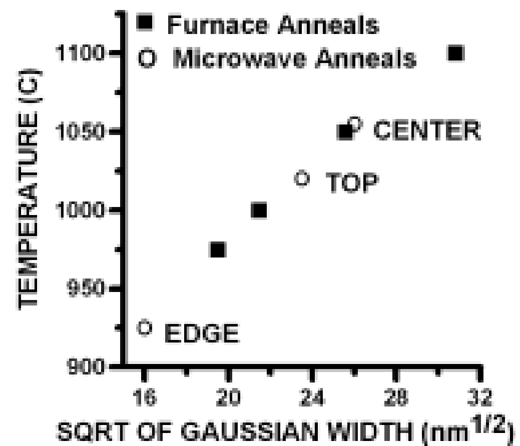

Figure 6. Plot of Temperature vs. the sqrt of the Gaussian Width from SIMS of the diffusion profiles. The wafer temperature in the microwave can be inferred by matching SIMS data to this plot.

THEORY

Electro-Magnetic Induced Heating, EMIH, is a unique application of Faraday's and Ampere's laws. When a silicon wafer is exposed to oscillating magnetic fields, currents -

more specifically electrons - are induced to flow within the wafer (Faraday's law). These electrons, through collisions with the lattice, give up their energy by heating the wafer.

Predicting the magnitude of these induced currents, however, requires a more detailed analysis of Faraday's and Ampere's laws. The currents induced in highly conducting materials, e.g. copper, re-induce a magnetic field that partially or completely interferes destructively with the incident field. This is commonly known as shielding or skin-depth. Conversely, the lack of free carriers in insulating materials, e.g. quartz, precludes any flow of current and allows the incident field to penetrate through the material. Semi-conductors fall in between these two extremes and therefore have the potential for significant field penetration that induces substantial currents throughout the volume of the wafer. This enables the possibility for *substantial and volumetric* heating, rather than just surface heating. This can be illustrated best by a self-consistent solution of Ampere's and Faraday's laws that obtains a first order description of induced current density and the subsequent power absorbed[8]:

$$P_{ABS} = \frac{\pi\, a^2 t_w^3 / \left(\delta^4 \sigma\right)}{1 + \left(t_w / \delta\right)^4} H_0^2 \quad , \qquad \delta = \sqrt{2/\omega\mu\sigma} \tag{1}$$

where σ is conductivity, t_w is thickness, δ is skin depth, ω is frequency, μ is permeability, "a" is radius, and H_o is the incident magnetic field. It is inferable from Eq.(1) that the absorbed power increases with conductivity, σ, until a peak absorption point is reached at which point the power decreases and asymptotes to zero, as shown in Fig 7a.

The strong dependence of power absorption on conductivity adds an elusive element to the heating of silicon because of the non-linear relationship between temperature and conductivity in a silicon wafer. This relationship is discussed in most fundamental semiconductor books[9] so only a brief summary is given here. Conductivity is the product of mobility and carrier density, but both these terms have opposing relationships with temperature. Mobility decreases with temperature due to an increased collision frequency that impedes the flow of carriers. Carrier density increases with temperature as the increased thermal energy moves more carriers from the valence band into the conduction band; thereby increasing the intrinsic carrier concentration. Empirical relationships that provide a quantitative description of these phenomena are readily available[9] and Fig 7b illustrates the dependence of conductivity on temperature for a variety of background doping concentrations.

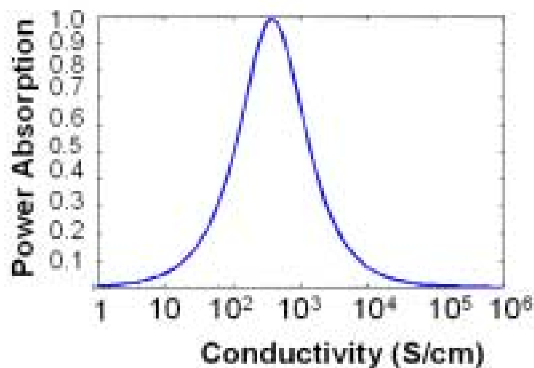

Figure 7a. Power absorption as a function of conductivity.

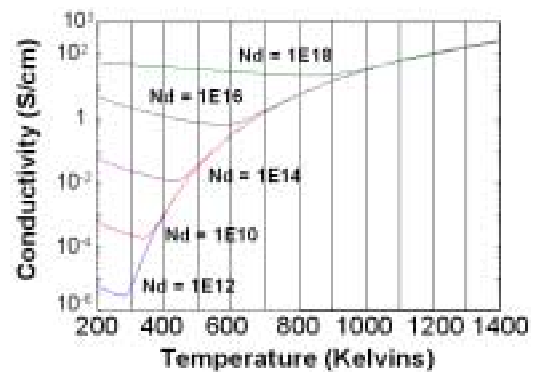

Figure 7b. Conductivity (S/cm) of an n-type silicon wafer for various levels of substate doping.

From Fig. 7, it is apparent that conductivity initially decreases with temperature - as collisions impede carrier mobility – until the temperature exceeds ~ 100°C. At this point the increase in intrinsic carriers overcomes the loss in mobility and conductivity increases monotonically with temperature. This gives several important results. First, a conductivity valley exists just above room temperature (50 – 125°C). This creates, due to the strong dependence of power absorption on conductivity, the possibility of an absorption valley which prevents the wafer from heating beyond ~ 100°C. Once beyond this point conductivity increases with temperature and power absorption increases with conductivity. This creates a runaway heating effect that results in extremely rapid temperature ramp rates. Next, above ~ 500°C the intrinsic carrier concentration becomes much greater than the background doping; consequently, the intrinsic carriers, not the specific wafer doping, dominate conductivity. Consequently, above 500°C wafer heating becomes independent of the initial substrate doping, and silicon wafers of various room temperature conductivities heat in an identical fashion.

EXPERIMENTAL RESULTS

Several wafers ranging from intrinsic (500 ohm-cm) to highly doped (.001 ohm-cm) and diameters from 2.5 cm to 10 cm were heated in both the microwave and RF systems. Rapid heating in the microwave system was successful without the need to pre-heat the wafers, but in the RF system, wafers with a bulk resistivity of 20 ohm-cm or greater required pre-heating to 150°C. This is not unexpected since higher frequency fields were expected to heat more efficiently and thus move through the coupling valley discussed in the THEORY section, while the RF fields were not able to do so. Furthermore, the heating rates above 500°C in both systems were independent of the room temperature wafer conductivity. The heating transient of an intrinsic, 10 cm wafer being heated at 1300 Watts in the microwave system is shown in Fig 8. The linear increase of temperature with time in this figure indicates that the response time of the pyrometer, ~ 125°C/sec, may be slower than the actual heating rate of the silicon wafer; giving a lower bound on the heating rate.

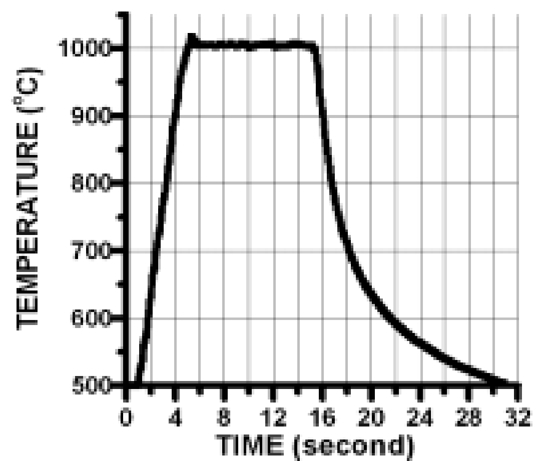

Figure 8. Temperature transient for heating an intrinsic (500 ohm-cm) silicon wafer in the μ–wave system

In this high temperature regime, the dominant loss mechanism is radiation from the wafer. When radiation losses equal the power absorbed from the electromagnetic fields, a steady state temperature is reached. Because power loss from radiation is governed by a fourth root dependence on temperature, steady state temperature is plotted as a function of power$^{1/4}$ in Fig.9. The data confirm that radiant heat transfer is the dominant thermal loss mechanism.

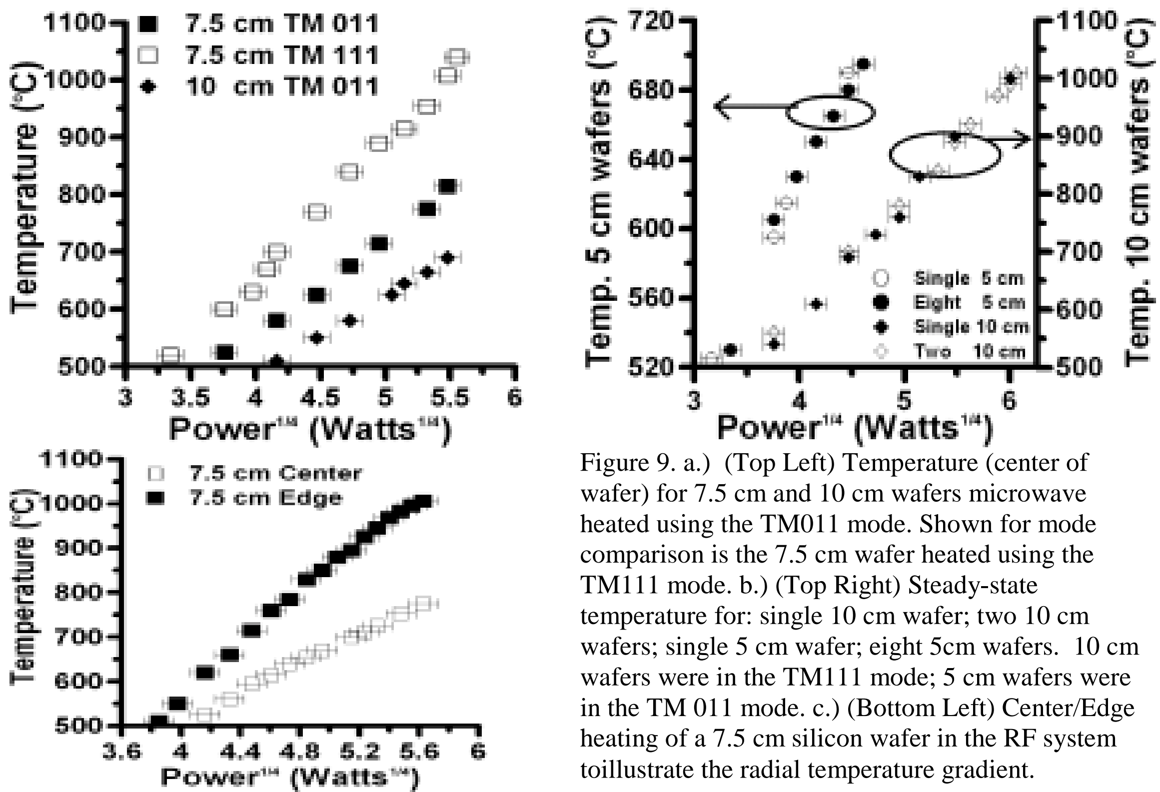

Figure 9. a.) (Top Left) Temperature (center of wafer) for 7.5 cm and 10 cm wafers microwave heated using the TM011 mode. Shown for mode comparison is the 7.5 cm wafer heated using the TM111 mode. b.) (Top Right) Steady-state temperature for: single 10 cm wafer; two 10 cm wafers; single 5 cm wafer; eight 5cm wafers. 10 cm wafers were in the TM111 mode; 5 cm wafers were in the TM 011 mode. c.) (Bottom Left) Center/Edge heating of a 7.5 cm silicon wafer in the RF system toillustrate the radial temperature gradient.

Figure 9a shows the temperature (measured in the wafer center) of single wafers heated in the μ–wave system in the TM011 mode. The center temperature data for a 7.5 cm wafer heated in the TM111 mode has been added to the plot to illustrate the difference in heating efficiency between the two modes. It can be inferred that the TM111 mode is more efficient for heating than the TM011 mode in these experiments (compare the 7.5 cm wafer TM111 and TM011 temperatures). The ability to perform batch processing is shown in Fig. 9b. For a given power, the same temperature is achieved for simultaneously heating several wafers or a single wafer. Finally, Fig 9c illustrates that with the present configuration, a radial temperature gradient is present in the RF system. This non-uniform temperature distribution results from a variation in induced currents across the wafer and is discussed in detail in another publication.[10] This is a significant issue for practical implementation, but alternative source designs have the potential for eliminating this gradient. Nevertheless, the preliminary data presented in this paper reveal the ability to rapidly heat wafers in the RF frequency regime.

Annealing several shallow-implanted samples provided by Varian Semiconductor Equipment Associates (VSEA) tested the effectiveness of EMIH for annealing ultra-shallow junctions. B^+ and BF_2^+ ions, at a dose of $10^{15}/cm^2$, were implanted into n-type <100> silicon wafers of resistivity 10-20 ohm-cm over a range of implant energies, 250 eV to 2.2keV. One additional sample was implanted using a new technology, PLAD[11] doping (BF_3 gas), also at a dose of $10^{15}/cm^2$.

These samples were spike annealed to either 900°C or 1000°C in both the RF and the μ–wave systems in an uncontrolled ambient at atmospheric pressure. Sheet resistances vs. junction depths evaluated at $10^{18}/cm^3$ from SIMS are plotted in Fig 10. The dashed line in Fig. 10 is the SEMATECH barrier[11] curve employed over the last couple of years as a benchmark[11] for evaluating improvements in anneal and doping technology. Data

points which fall below (south-west of) this curve indicate improvement on this current standard since it represents a higher percentage of activated dopants and/or a more efficient annealed dopant profile (i.e. a more "box-shaped" profile). Also plotted is the most recent data (taken by Lerch et. al.[12]) of samples spike annealed at 425°C/sec with a cool rate of 120°C/sec in an optimized nitrogen and oxygen ambient.

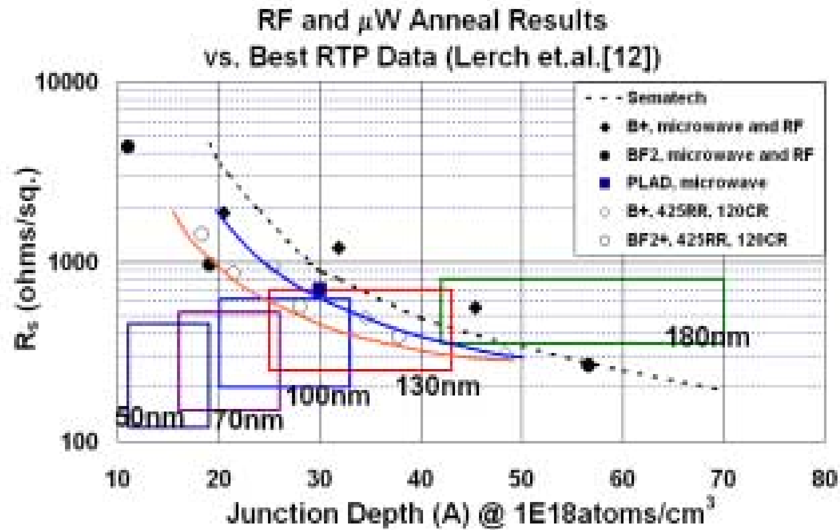

Figure 10. Sheet resistance vs. junction depth to compare EMIH anneal results against SEMATECH technology barrier and best results to date. Points falling below the SEMATECH line represent improvement in either dopant activation or

Illustrative SIMS results for the as-implanted and microwave spike annealed PLAD samples are shown in Fig. 11. Because the PLAD implant utilizes a BF_3 source gas, it compares more closely[11] to the BF_2 beam implants. The PLAD data point shows remarkably little diffusion, ~ 10nm, for its resultant sheet resistance value of 700 ohms/square. This data point, along with the three BF_2 implants fall below the SEMATECH line, especially at the shallow junction end, and follow the same curve as the data taken by Lerch et.al.[12] Lerch et al.[12] have also demonstrated that BF_2 implants, after undergoing RTA, are more efficient in both dopant profile (i.e. more box shaped) and in dopant activation compared to B implants. EMIH anneals agree with this correlation. Further optimization and improvement for the RF and microwave annealed wafers should come by: controlling the ambient during anneal, increasing ramp and cool rates, and perhaps with further optimization of the anneal temperature. It has been shown[2,3,4] that a controlled ambient of 33 ppm oxygen eliminates the oxygen-enhanced-diffusion effect while growing just enough of a thin oxide layer to hinder boron out-diffusion from the wafer. This results in significantly less diffusion – yielding a more efficient profile - and an increased dose retention during the anneal process. By comparing to SIMS profiles done in conventional RTA systems[3], it is estimated that a potential reduction in junction depth of 15% is possible by controlling the EMIH ambient in a similar fashion. Additional improvements are obtainable by increasing the heating and cooling rates[12]. These optimizations should satisfy the 100 nm benchmark and may be enough to satisfy the 70 nm benchmark.

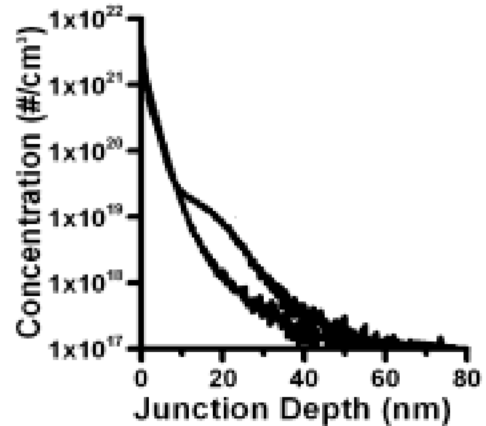

Figure 11. SIMS profile from PLAD implant at 1keV, dose of $10^{15}/cm^2$ Resulting Rs was 700 ohms/square

CONCLUSION

A novel heating technique, EMIH, has been introduced which appears to satisfy the SEMATECH benchmark for 100 nm processing and has the strong potential, with optimizations, to satisfy the 70 nm benchmark as well. This process also has the potential for bulk processing. Because the equipment used in these experiments is standard in modern manufacturing facilities, integration into existing process lines would have the advantage of incorporating previous operational and maintenance experience. Further studies will investigate annealing in a controlled ambient, improved source design for RF annealing, and multi-mode or over-moded microwave cavity designs.

ACKNOWLEDGEMENTS

The authors would like to thank Susan Felch, and Ziwei Fang of VSEA for providing the PLAD wafers and for performing the sheet resistance measurements: a special thanks to Edwin Arevalo also of VSEA for assistance with the implants and many of the post anneal analysis. Further thanks to David Sing and Joe Bennet of SEMATECH for additional SIMS analysis. This research was made possible in part by award no. RE1-2065 of the U.S. Civilian Research and Development Foundation for the independent states of the former Soviet Union (CRDF), and through sponsorship by the University-Industrial Relations Office of the University of Wisconsin.

REFERENCES

1. Packan, P. “Scaling Transistors into the Deep Submicron Regime”, *MRS Bulletin*. June 2000. pp. 18 - 21
2. D.F. Downey, S.B. Felch, and S.W. Falk, “Doping and Annealing Requirements to Satisfy the 100nm Technology Node”, *Proc. of the Electro-Chemical Society, May 1999*. (Seattle, WA 1997)
3. D.F. Downey, J.W. Chow, W. Lerch, J. Niess, S. D. Marcus; *Proceedings of MRS-Rapid Thermal and Integrated Processing VII, Vol. 525*. April 1998, pp 263-271
4. D.F. Downey, S. W. Falk, S.D. Marcus; Proc. of 7TH International Conference on Advanced Thermal Processing of Semiconductors, 1999, pp 229-236
5. K. Thompson, J.H. Booske, R.F. Cooper, Y.B. Gianchandani, *Proceedings of Selected Papers from the Second World Congress on Microwave Processing*, 2-6 April, 2000
6. Accufiber operating Manual, Luxtron Corporation. (1989)
7. R.C. Jaeger. Introduction to Microelectronic Fabrication. Addison Wesley: Reading Massachusetts. (1993)
8. Shen, L.C. Kong, J.A. Applied Electromagnetism. PWS Publishing: Boston, Massachusetts. p.552. (1995)
9. R.F. Peirret. Advanced Semiconductor Fundamentals. Addison Wesley: Reading, Massachusetts. (1989)
10. Keith Thompson, Yogesh B. Gianchandani, John Booske, Reid Cooper ,11th International Conference on solid-state sensors and actuators, 10 June 2001, Munich, Germany.
11. R.B. Liebert, S.R. Walther, S.B. Felch, Z.Fang, B.O. Pedersen, D. Hacker. “Plasma Doping System for 200 and 300 mm Wafers”, to be published in the Proc. of Ion Implant Technology 2000.
12. W. Lerch, B. Bayha, D.F.Downey, E.A. Arevalo; “State of the Art Techniques for Ultra-shallow Junction Formation” presented at ECS March 2001 and published in this Proceeding.